Case Report

Imaging performance of thoracic SMARCA4-deficient undifferentiated tumor: a case report and literature review

Di Yang, Yong Wang

Department of Ultrasound, National Cancer Center, National Clinical Research Center for Cancer, Cancer Hospital, Chinese Academy of Medical Sciences and Peking Union Medical College, Beijing, China

Contributions: (I) Conception and design: D Yang; (II) Administrative support: Y Wang; (III) Provision of study materials or patients: Y Wang; (IV) Collection and assembly of data: D Yang; (V) Data analysis and interpretation: D Yang; (VI) Manuscript writing: Both authors; (VII) Final approval of manuscript: Both authors.

Correspondence to: Yong Wang, MD. Department of Ultrasound, National Cancer Center, National Clinical Research Center for Cancer, Cancer Hospital, Chinese Academy of Medical Sciences and Peking Union Medical College, Panjiayuan Nanli #17, Chaoyang District, Beijing 100021, China. Email: drwangyong77@163.com.

Background: SMARCA4-deficient undifferentiated tumor (SMARCA4-UT) is a class of high-grade malignant tumors that has only been described in recent years, with an undifferentiated or rhabdoid morphology and genetic deletion of *SMARCA4* (*BRG1*), a subunit of the *BRG1*-associated factors (BAFs) chromatin remodeling complex. It is a rare tumor type that occurs in young to middle-aged men and usually presents as a compressive thoracic mass with rapid progression and poor prognosis. However, much remains unknown about the clinical and imaging manifestations of the disease.

Case Description: Herein, we report a 51-year-old man who came to our hospital with multiple enlarged lymph nodes in the chest after a computed tomography (CT) examination at another hospital. The patient underwent conventional ultrasound (US), contrast-enhanced ultrasound (CEUS), magnetic resonance imaging (MRI), ^{18}F-fluorodeoxyglucose positron emission tomography/CT (PET/CT), and finally confirmed the diagnosis of SMARCA4-UT by US-guided puncture biopsy. After symptomatic management, the patient was transferred to another hospital and we performed a short-term follow-up.

Conclusions: During this procedure, we obtained a series of relevant clinical and imaging data, especially US and CEUS images, which were described for the first time, offering valuable imaging information that will contribute to the clinical diagnosis of this disease to a certain extent. Moreover, this case highlights the efficacy of CEUS in identifying internal necrosis within tumors and lymph nodes, thereby improving the success rate of obtaining tumor tissue for pathological diagnosis. These findings substantiate the practical utility of US and CEUS in the context of mediastinal SMARCA4-UT, emphasizing their potential for widespread clinical adoption.

Keywords: *SMARCA4*; mediastinum neoplasms; image performance; ultrasonography; case report

Submitted Dec 12, 2023. Accepted for publication Jan 31, 2024. Published online Feb 28, 2024.
doi: 10.21037/tlcr-23-822
View this article at: https://dx.doi.org/10.21037/tlcr-23-822

Introduction

In 2015, Le Loarer *et al.* (1) first described aggressive thoracic tumors with defects in *SMARCA4*, the ATPase subunit encoding the *BRG1*-associated factors (BAFs) chromatin remodeling complex, which plays an important role in transcription, differentiation, and DNA repair. The transcriptional profiles of these tumors appear to be more similar to malignant rhabdoid tumors yet harbor a specific "immunohistochemical signature": co-loss of *SMARCA4* and *SMARCA2* with overexpression of *SOX2* (2). Thus,

the term "thoracic SMARCA4-deficient undifferentiated tumor" has been added to other epithelial tumors in the World Health Organization (WHO) Classification of Thoracic Neoplasms, 2021 edition (3,4). Clinically, several clinicopathological series have shown that these tumors have a male predominance and tend to occur in younger to middle-aged patients. And it is revealed as primarily smoking-related (5-7). Besides, this novel class of exceptionally aggressive thoracic tumors has a dismal prognosis, with a median survival of about 7 months (8). The diagnosis of SMARCA4-deficient undifferentiated tumor (SMARCA4-UT) is essential due to the different treatment and prognosis from those of other thoracic malignancies. However, it has been found to have atypical clinical symptoms and little imaging information, and the imaging diagnosis of this disease is still a challenge. In addition, no one has previously described the presentation of SMARCA4-UT by ultrasound (US) and contrast-enhanced ultrasound (CEUS) imaging. To improve the imaging knowledge related to SMARCA4-UT, we report this unusual case and review the relevant literature. We present this case in accordance with the CARE reporting checklist (available at https://tlcr.amegroups.com/article/view/10.21037/tlcr-23-822/rc).

Highlight box

Key findings

- This is the first report of SMARCA4-deficient undifferentiated tumor (SMARCA4-UT) ultrasound (US) and contrast-enhanced ultrasound (CEUS) images of the chest.

What is known and what is new?

- SMARCA4-UT is a rare, highly malignant thoracic tumor recently identified in young to middle-aged men, associated with a history of smoking, and characterized by rapid progression and poor prognosis.
- The study emphasizes the challenges in clinical diagnosis and highlights the significance of US and CEUS in providing special imaging features. The study contributes valuable information for improving the imaging-based diagnosis of this rare and aggressive thoracic tumor, underscoring the utility of CEUS in detecting internal necrosis and aiding in successful pathological diagnosis.

What is the implication, and what should change now?

- The novel insights into imaging features, particularly the utility of US and CEUS, suggest that incorporating these techniques into the diagnostic workflow can enhance the accuracy of identifying SMARCA4-UT. This learning can influence the choice of imaging modalities in suspected cases.

Case presentation

A 51-year-old man reported shoulder and posterior back pain for 2 weeks, with numbness in both lower limbs and unsteady gait for 3 days. The patient first underwent a computed tomography (CT) examination at another hospital, indicating that multiple soft tissue occupations in the left supraclavicular region, anterior superior mediastinum and subpleural of the left upper lobe of the lung, multiple lymph nodes enlargement in the mediastinum, destruction of the third and fourth ribs on the left side, considering malignant lesions, inclining to lymphoma. The patient had a history of smoking for approximately 30 years. Physical examination showed that the patient was generally weak but had normal basic signs. He was unable to walk alone, and multiple enlarged lymph nodes can be palpated in the neck. Tumor marker test results revealed neuron-specific enolase (NSE) was 54.83 ng/mL (reference range, 0.0–16.3 ng/mL). Conventional US, CEUS, magnetic resonance imaging (MRI), and ^{18}F-fluorodeoxyglucose (FDG) positron emission tomography/computed tomography (PET/CT) were performed for imaging assessment.

The initial conventional US was used to evaluate the position and characteristics of superficial lymph nodes and determine whether US-guided lymph node aspiration biopsy can be performed. Plenty of enlarged lymph nodes were detected on both sides with abnormal morphology. The largest of these lymph nodes had a maximum cross-section of 4.1 cm × 2.5 cm (*Figure 1A*). The shape of these lymph nodes was round or oval or irregular with increasing short diameter, fused partially, the cortex of them was markedly thickened, some of the margins were not clear, and the lymphatic portal structures were eccentric or disappeared. Color Doppler showed that the lymph nodes contained disorderly dotted and striped blood flow signals around and inside them (*Figure 1B*). Notably, the patient suffered a severe ache around the scapula, so an ultrasonographic examination was also performed on his back, revealing a hypoechoic mass in the left posterior mediastinum. With a maximum cross-section of 7.0 cm × 3.8 cm, the mass had an irregular shape and unclear margin (*Figure 1C*).

To observe the internal condition of the enlarged lymph nodes and posterior mediastinal mass to guide the puncture, ultrasonography was performed on his largest cervical lymph nodes and posterior mediastinal space occupancy with the patient's informed consent. CEUS image exhibited that the largest lymph node was enhanced at 10 s, with rapid

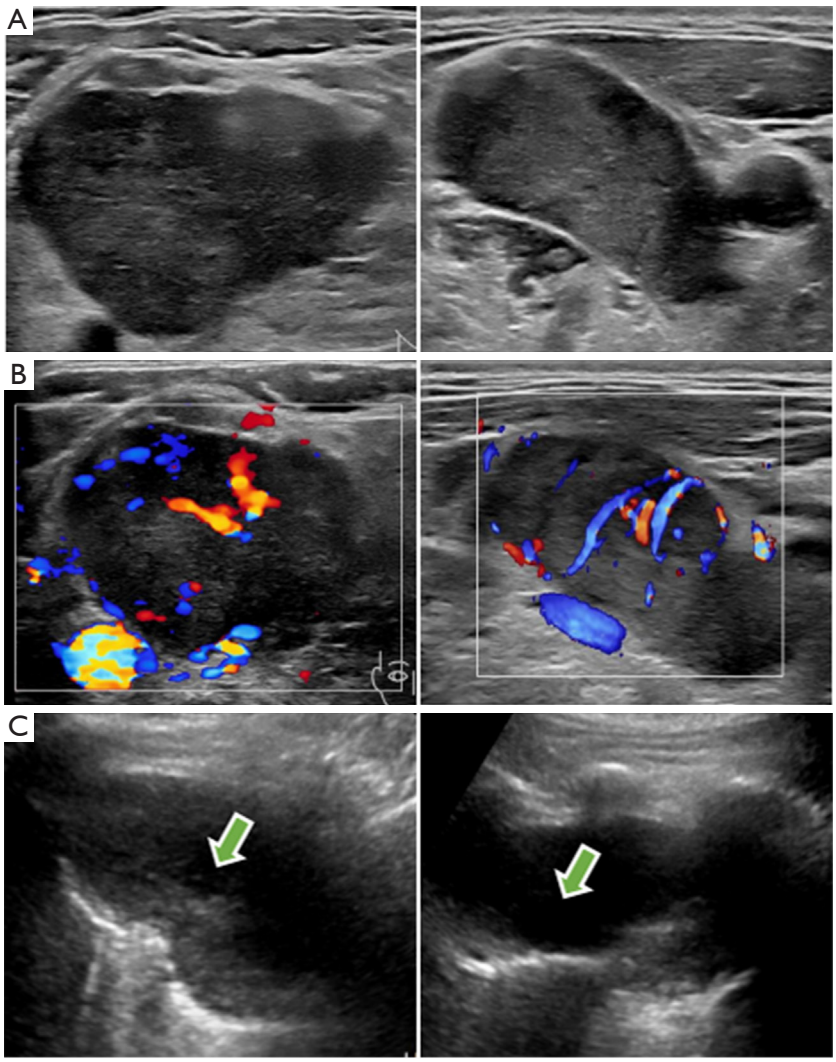

Figure 1 Two-dimensional ultrasound images of cervical lymph nodes and mediastinal masses. (A) Two-dimensional ultrasound images of enlarged lymph nodes in the right and left neck. (B) Color Doppler ultrasound images of enlarged lymph nodes in the right and left neck. (C) Two-dimensional ultrasound shows transverse and longitudinal views of the posterior mediastinal mass, with an echogenic area seen inside (green arrows).

dendritic hyperperfusion from the periphery toward the center, reaching the peak enhancement at 18 s (*Figure 2A*). The peak intensity was 4.53 dB and a quick contrast withdrawal time and a peak drop of 50% for about 12 s were observed (*Figure 2B*). Whilst the CEUS of the posterior mediastinal space showed that the mass began to enhance at about 11 s, showing a high enhancement pattern in the peripheral solid area, and reached the peak enhancement at 46 s with a peak intensity of 19.55 dB (*Figure 2C*), with a large non-enhancing area inside the tumor, and a continuous isoenhancing pattern in the peripheral enhancement area at a later stage, with a peak decrease of 50% at about 179 s (*Figure 2D*).

The T2-weighted image of MRI showed a tumor located in the posterior mediastinum with a maximum diameter of approximately 7.0 cm × 6.5 cm, which presented as a fusion of multiple masses encompassing and infiltrating the connective tissue and bony structures of the cervico-thoracic region (*Figure 3A*). T2 and T3 corresponded to spinal canal stenosis and spinal cord compression signal changes, with a length of about 3.6 cm and unclear borders, and local cerebrospinal fluid flow was blocked (*Figure 3B*).

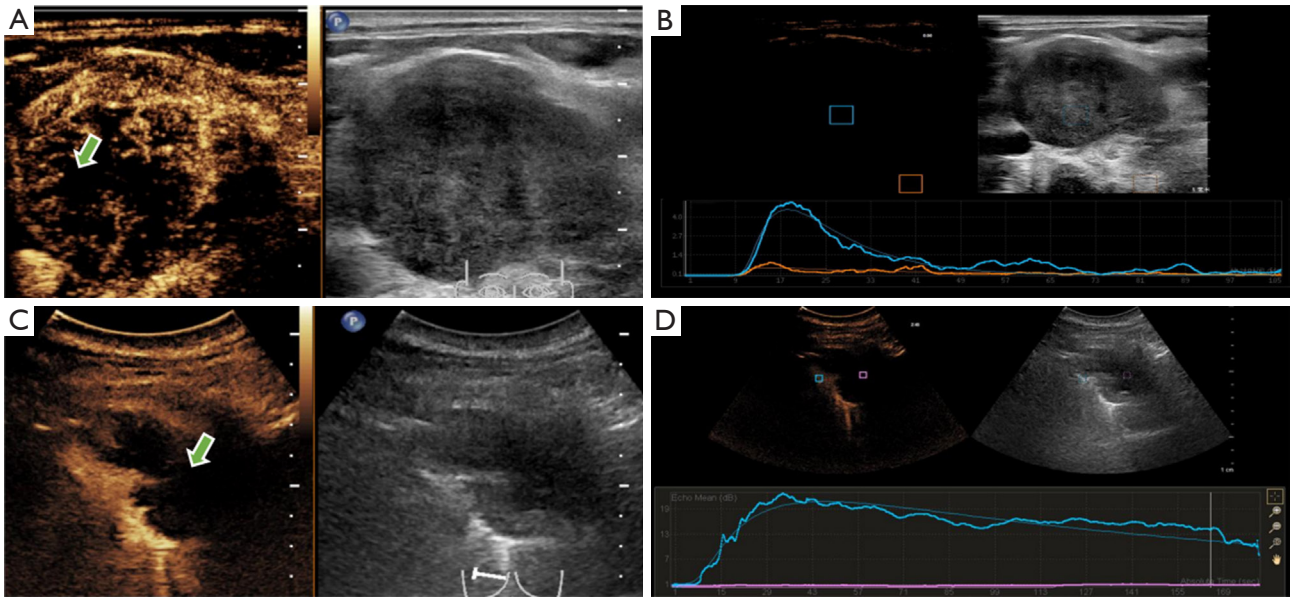

Figure 2 CEUS images of cervical lymph nodes and mediastinal masses. (A) CEUS and US images of the right cervical enlarged lymph node at the peak at 18 s, with a restricted non-enhancing area inside (green arrow). (B) Peak-intensity curve of CEUS of the enlarged lymph node in the right neck. Blue line: an enhanced area within the lymph node; orange line: surrounding normal soft tissue. (C) CEUS and US images of the posterior mediastinal mass at the peak at 46 s, with a large area of no enhancement seen inside (green arrow). (D) Peak-intensity curve of CEUS of posterior mediastinal mass. Blue line: solid enhancing area around the tumor; pink line: no enhancing area inside the tumor. CEUS, contrast-enhanced ultrasound; US, ultrasound.

^{18}F-FDG PET/CT showed a left posterior mediastinum and intravertebral canal mass with irregular nodular growth along the posterior costal pleura and mediastinal pleura with unevenly increased uptake, with a maximum standardized uptake value (SUV) of 12.0 (*Figure 3C*,*3D*). The mass encircled the left ribs and involved the thoracic vertebrae, with localized visible bone destruction. In addition, multiple nodules and masses with increased uptake in the bilateral neck, mediastinum, and left hilum, with a maximum SUV of 14.9, partially fused into a mass. Emphysema and multiple pulmonary alveoli were also seen in the right lung (*Figure 4A*). The axial, coronal, and sagittal maximum intensity projection (MIP) images centered on the lesion provided a more complete picture of the location of the disease and its relationship to surrounding tissue structures (*Figure 4B-4D*). Combined with the above PET/CT considered a malignant tumor and gave a diagnostic tendency of malignant tumor of mesenchymal origin (malignant nerve sheath tumor or malignant neurofibroma), neuroendocrine carcinoma with multiple metastases, and lymphoma.

The patient was screened for viral indicators before undergoing a puncture biopsy at our hospital, and was not found to be infected with human immunodeficiency virus (HIV), syphilis, or hepatitis B and C viruses, and there was no history of previous surgeries or genetic disorders. Subsequently, pathological findings were obtained from the largest lymph node in the left supraclavicular region and the posterior mediastinal mass by US-guided histological biopsy. The results showed malignant tumor cells in the lymph node and in the posterior mediastinal area with a tendency of poorly differentiated cancer cells, and histopathology revealed largely grayish-white fragmented tissue, and pathology showed a malignant tumor with necrosis. Combined with immunohistochemical results, SMARCA4-UT was finally identified. Immunohistochemical results revealed AE1/AE3 (–), Syn (3+), ChrA (–), Ki-67 (+, 70%), CK18 (–), SALL4 (3+), Oct3/4 (–), LCA (–), CD56 (–), SOX10 (–), SOX2 (3+), CD99 (1+), INI1 (+), BRG1 (–), CD34 (–), P53 (3+). Genetic testing revealed mutations in exon seven of the *SMARCA4* gene.

During this time the clinician provided general treatment with fluid replacement, pain relief, and lowering of cranial pressure. After the diagnosis was made, the patient opted

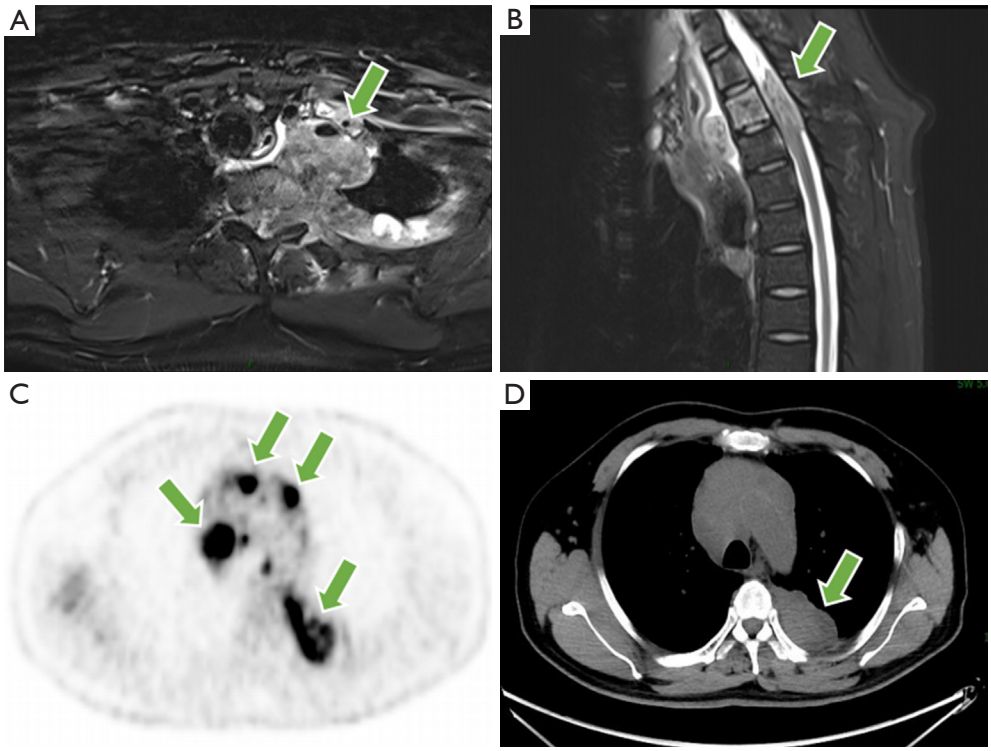

Figure 3 MRI and ^{18}F-fluorodeoxyglucose PET/CT images of the mediastinal masses. (A) MRI T2-weighted image shows multiple cervicothoracic, mediastinal, and pleural masses fused (green arrow). (B) The mass encircles the surrounding blood vessels and invades the vertebral body, and the T2 and T3 vertebrae correspond to spinal stenosis and spinal cord compression (green arrow). (C) PET/CT shows increased multiple uptakes in the mediastinum and left hilum (green arrows). (D) CT image of the elevated area corresponding to the posterior mediastinal mass was taken (green arrow). MRI, magnetic resonance imaging; PET/CT, positron emission tomography/computed tomography; CT, computed tomography.

to return to the local hospital for palliative care and was followed up by telephone 2 weeks later, at which the patient was generally stable.

All procedures performed in this study were in accordance with the ethical standards of the institutional and/or national research committee(s) and with the Helsinki Declaration (as revised in 2013). Publication of this case report and accompanying images was waived from patient consent according to the institutional review board of National Cancer Center/Cancer Hospital, Chinese Academy of Medical Sciences and Peking Union Medical College.

Discussion

SMARCA4-UT has been named SMARCA4-deficient thoracic sarcoma and SMARCA4-deficient thoracic sarcoma-like tumor. In 2019, Perret *et al.* (7) in France proposed three criteria that should lead to the diagnosis of SMARCA4-deficient thoracic sarcoma: (I) a transverse muscle or poorly differentiated phenotype; (II) complete loss of expression of *SMARCA4* and *SMARCA2*; (III) focal or diffuse expression of at least two of *SOX2*, *CD34* or *SALL4*. Thoracic SMARCA4-UTs frequently express "stem cell markers" such as *CD34*, *SALL4*, and *SOX2*, and synaptophysin expression is common. In the present case, it meets the above diagnostic criteria, and immunohistochemistry showed that the tumor contained synaptophysin expression, indicating that the tumor cells may have neuroendocrine properties. Meanwhile, in recent years researchers have found that the cytology of SMARCA4-UT is characterized by atypical round or polygonal cells that appear singly or in loose clusters, and some cells demonstrating rhabdoid morphology, with convoluted nuclei, prominent nucleosomes and binucleated and multinucleated forms set in a necrotic

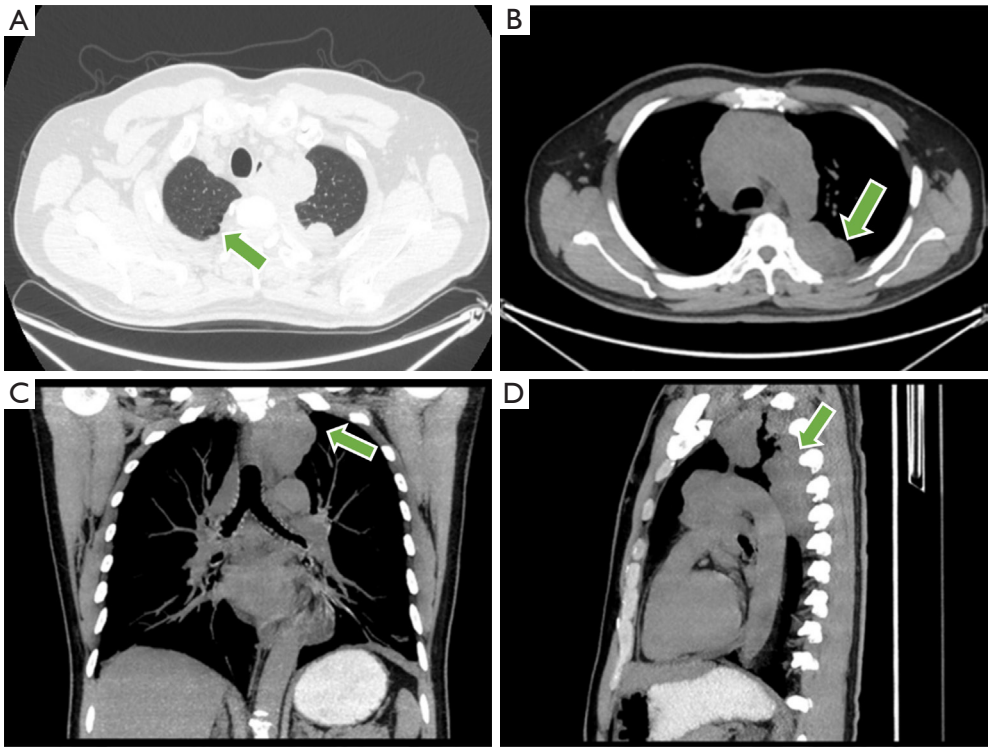

Figure 4 Computed tomography and MIP images of the patient. (A) Presence of a limited distribution of rounded, wall-less hypodense areas in the subpleural of the apical segment of the right upper lobe of the patient's lungs (green arrow). (B) Axial bit MIP image displayed a large mass in the mediastinum left pleura region, invading the rib on the left, soft tissues around the left posterior upper back (green arrow). (C) The coronal MIP image showed the mass as an irregular nodule, encircling the large mediastinal pericardial vessels (green arrow). (D) The sagittal MIP image showed the mass involved in the aorta and multiple thoracic vertebrae (green arrow). MIP, maximum intensity projection.

background (9,10). The above manifestations reflect its highly malignant state, it is highly progressive and invasive, and the imaging manifestations in this case, such as the large tumor volume, showing infiltrative growth, extrusion destroying the surrounding tissues and organs and large necrotic areas inside the lesion, are also consistent with its histopathological features.

In terms of clinical presentation, with rapidly progressive intrathoracic tumors often pushing surrounding tissues, patients often have symptoms attributable to a large compressive mediastinal mass, with or without lung involvement, and may also present with symptoms of distant metastasis. Affected patients are typically smokers, and emphysema is often notable even in young patients, which has led some to postulate that patients at risk for this malignancy may have a particular susceptibility to smoking-related lung damage (11). This case had a history of smoking for approximately 30 years and imaging of smoking-related lung injury, such as emphysema and pulmonary maculopathy, consistent with the epidemiological features of this tumor.

So far, SMARCA4-UT has shown a poor response to conventional chemotherapy regimens, and now bromodomain inhibitors, *EZH2* inhibitors and immune checkpoint inhibitors are currently being used in clinical trials (12-16). These emerging drugs have the potential to improve prognosis for SMARCA4-UT patients but results need to be validated in a larger population.

SMARCA4-UT behaves aggressively and has a worse prognosis compared with other poorly differentiated thoracic tumors such as *BRG1*-retained tumors and thymic carcinoma. Therefore, the identification of SMARCA4-UT is important for both prognosis and treatment. A multicenter study of 21 patients found that the majority of SMARCA4-deficient thoracic sarcomas presented on CT as compressive and infiltrative chest masses extending from the mediastinum to multi-compartment extension

of lung apex, pleura, or neck with ill-defined necrotic lymph nodes, and primary tumors exhibit strong FDG avidity on PET/CT scan (17). SMARCA4-deficient non-small cell lung cancer (NSCLC), which has emerged as a unique subgroup of NSCLC only in recent years, is also characterized by highly aggressive growth, and SMARCA4-deficient NSCLC accounts for only 3% to 6% of all NSCLC compared to SMARCA4-intact NSCLC, which is larger at the time of discovery, and more adrenal and lymph node metastases are present. However, SMARCA4-deficient NSCLC usually presents as a primary solid lung mass, with a prevalence of upper lobe and peripheral lung tumors, and is associated with pericardial, brain, and hepatic metastases, and emphysema has not been reported in many patients (18). It has also been shown that tumor necrosis is more pronounced in SMARCA4-UT than in SMARCA4-deficient NSCLC, and the same performance is also observed in the image of our case (19). In the present patient, MRI and PET/CT showed an all-round infiltrative growth of the tumor into the cervical lymph nodes, mediastinal regions, pleura, cervicothoracic and pericardial vessels, ribs, spine and muscular and soft tissues of the thoracic back, reflecting its highly aggressive nature. The tumor imaged by ^{18}F-FDG-PET/CT also demonstrated a strong metabolic activity. In addition, SMARCA4-UT often showed marked necrosis (20). It should be suspected if the chest mass is large, heterogeneous, and exhibits infiltration and compression of surrounding tissues, accompanied by necrotizing lymphadenopathy (21). And CEUS has an excellent ability to detect internal necrosis in tumors and lymph nodes (22,23).

Given the imaging presentation of SMARCA4-UT and the fact that the patient also had elevated levels of NSE, it is easy to misdiagnose as other mediastinal malignancies, such as lymphoma, neuroendocrine tumors (NETs), and neurogenic tumors. PET/CT has become the technique of choice for staging and follow-up in patients with extra-nodal involvement in Hodgkin's disease and most cases of non-Hodgkin lymphomas (24). On FDG-PET, malignant lymphomas are FDG-avid with typical SUVmax values of greater than 6.0 (25). Radiographically, the presentation of primary NET is atypical, presenting as ill-defined lobulated homogenously moderately enhancing mass in the anterior mediastinum. Lymphadenopathy, metastasis to the liver, lung, pancreas, pleura, and bone, and infiltration to adjacent vascular structures are also common (26). And according Ozawa *et al.* (27), neurofibromas show similar CT findings to schwannomas. Both are well-defined, smooth, oval, or round masses that appear as isointense contrast enhancement relative to the muscle. Nevertheless, MRI findings are slightly different between the two. The interior of schwannomas is more likely to show cystic changes or hemorrhage, whereas the "target sign"—characterized by a low central signal intensity and a high peripheral signal intensity—is more common in neurofibromas (28). However, the imaging presentation of these diseases is not specific and is currently used only for the staging and risk assessment of the disease (29,30). In small cell lung cancer (SCLC), which is also prevalent in heavy smokers, the most common imaging manifestation is a large hilar mass with massive mediastinal lymph node enlargement, characterized by a central airway infiltration of the submucosal layer and progressive narrowing of the bronchial lumen through outward or endobronchial spread, with a particular tendency for SCLC to spread to the liver, adrenal glands, bone, bone marrow, and brain. Microscopically, it showed a characteristic pike or oatmeal shape, diffusely distributed or lamellar, with cells about twice the size of lymphocytes, which could be differentiated from the present case on the basis of imaging features and histopathologic manifestations (31,32). In addition, for the equally rare and highly aggressive nuclear protein in testis (NUT) carcinoma, it has been reported that it is more common in young people, with a median age at diagnosis of 16–30 years old, and a roughly equal incidence in both sexes (33). Imaging findings often involve the patient's midline structures, such as the mediastinum, upper airway, and upper gastrointestinal tract, with those with chest involvement often presenting with symptoms of cough, dyspnea, or bone pain due to bone metastases, which are similar to some of the symptoms in this case. However, patients with NUT carcinoma usually do not have a significant history of smoking, and there is no evidence that patients are often accompanied by emphysema. Immunohistochemical detection of NUT protein has a high sensitivity and specificity for the diagnosis of this disease, so relatively extensive immunohistochemical testing is still needed to aid in its differential diagnosis from SMARCA4-UT (34,35).

Due to the effects of air in the lungs and occlusion of the bony structures of the thorax, US has limited value for diagnostic imaging and differential diagnosis of mediastinal occupations, and has little clinical use. Some studies have summarized the US characteristics of mediastinal occupations by transthoracic US, such as pericardial cysts and thymic cysts usually show anechoic occupations with good sound transmission, teratomas often show mixed

echogenic masses, and benign thymomas often show round or oval hypoechoic masses with clear borders and homogeneous internal echogenicity, while malignant thymic carcinomas, etc., often show non-smooth membranes with unclear borders and inhomogeneous internal echogenicity. In contrast, malignant thymic carcinoma often shows a hyperechoic occupancy with an unsmooth periphery, unclear border and uneven internal echoes. In addition, mediastinal lymphoma is often a well-defined hypoechoic mass with multiple fusions on US (36,37). Regarding the CEUS presentation of mediastinal tumors, Pan *et al.* (38) found the specificity of CEUS was higher than that of contrast-enhanced MRI (CE-MRI), and the positive predictive value and diagnostic coincidence rate of CEUS were equal to those of CE-MRI, which means CEUS can be used as an effective alternative and complementary examination for patients who cannot undergo CE-MRI. Kong *et al.* (39) summarized the ultrasonographic features of mediastinal lymphomas and found that thymomas often show homogeneous late enhancement with a low rate of internal necrosis. In contrast, late inhomogeneous centripetal enhancement features were more common in thymic carcinomas with a high rate of internal necrosis. And 57.6% of the enhancements of lymphomas began after 10 s, and 93.3% of them showed small areas of necrosis. In contrast, CEUS in the present case showed that tumor enhancement also began after 10 s, but presented a distinct ring-like enhancement with large internal necrosis.

For the histopathological examination of thoracic tumors, biopsy samples are often too small to make an exact diagnosis (40). For SMARCA4-UT, the diagnosis is particularly challenging due to the large number of necrotic biopsies within the tumor that are not easily accessible to tumor tissue. Hence, determining the active area of the tumor by CEUS increases the success rate of obtaining a pathological diagnosis with satisfactory safety and accuracy (41-43).

Conclusions

In summary, no specific imaging features have been identified for this disease and therefore a comprehensive clinical-imaging-pathological-genetic diagnosis is essential for the diagnosis of SMARCA4-UT. The case we present demonstrates a comprehensive imaging presentation of thoracic SMARCA4-UT and enriches the imaging knowledge, especially in terms of US and CEUS. It was also demonstrated that after identifying the active site of the tumor by CEUS, US-guided aspiration biopsy could effectively obtain tumor tissue for pathological diagnosis.

Acknowledgments

Funding: This work was supported by the National Natural Science Foundation of China (No. 81974268).

Footnote

Reporting Checklist: The authors have completed the CARE reporting checklist. Available at https://tlcr.amegroups.com/article/view/10.21037/tlcr-23-822/rc

Peer Review File: Available at https://tlcr.amegroups.com/article/view/10.21037/tlcr-23-822/prf

Conflicts of Interest: Both authors have completed the ICMJE uniform disclosure form (available at https://tlcr.amegroups.com/article/view/10.21037/tlcr-23-822/coif). The authors report that funding for this study was granted by the National Natural Science Foundation of China to cover the article processing charges of this paper. The authors have no other conflicts of interest to declare.

Ethical Statement: The authors are accountable for all aspects of the work in ensuring that questions related to the accuracy or integrity of any part of the work are appropriately investigated and resolved. All procedures performed in this study were in accordance with the ethical standards of the institutional and/or national research committee(s) and with the Helsinki Declaration (as revised in 2013). Publication of this case report and accompanying images was waived from patient consent according to the institutional review board of National Cancer Center/Cancer Hospital, Chinese Academy of Medical Sciences and Peking Union Medical College.

References

1. Le Loarer F, Watson S, Pierron G, et al. SMARCA4 inactivation defines a group of undifferentiated thoracic malignancies transcriptionally related to BAF-deficient sarcomas. Nat Genet 2015;47:1200-5.
2. Mardinian K, Adashek JJ, Botta GP, et al. SMARCA4: Implications of an Altered Chromatin-Remodeling Gene for Cancer Development and Therapy. Mol Cancer Ther 2021;20:2341-51.
3. Gantzer J, Davidson G, Vokshi B, et al. Immune-Desert Tumor Microenvironment in Thoracic SMARCA4-Deficient Undifferentiated Tumors with Limited Efficacy of Immune Checkpoint Inhibitors. Oncologist 2022;27:501-11.
4. Nicholson AG, Tsao MS, Beasley MB, et al. The 2021 WHO Classification of Lung Tumors: Impact of Advances Since 2015. J Thorac Oncol 2022;17:362-87.
5. Sauter JL, Graham RP, Larsen BT, et al. SMARCA4-deficient thoracic sarcoma: a distinctive clinicopathological entity with undifferentiated rhabdoid morphology and aggressive behavior. Mod Pathol 2017;30:1422-32.
6. Rekhtman N, Montecalvo J, Chang JC, et al. SMARCA4-Deficient Thoracic Sarcomatoid Tumors Represent Primarily Smoking-Related Undifferentiated Carcinomas Rather Than Primary Thoracic Sarcomas. J Thorac Oncol 2020;15:231-47.
7. Perret R, Chalabreysse L, Watson S, et al. SMARCA4-deficient Thoracic Sarcomas: Clinicopathologic Study of 30 Cases With an Emphasis on Their Nosology and Differential Diagnoses. Am J Surg Pathol 2019;43:455-65.
8. Yoshida A, Kobayashi E, Kubo T, et al. Clinicopathological and molecular characterization of SMARCA4-deficient thoracic sarcomas with comparison to potentially related entities. Mod Pathol 2017;30:797-809.
9. Takeda M, Tani Y, Saijo N, et al. Cytopathological Features of SMARCA4-Deficient Thoracic Sarcoma: Report of 2 Cases and Review of the Literature. Int J Surg Pathol 2020;28:109-14.
10. Punjabi LS, Lim KL, Chow CY, et al. Three shades of an unusual mediastinal tumour. Diagn Cytopathol 2023;51:716-23.
11. Boland JM. Unusual lung tumors-from morphology to genetics. Mod Pathol 2022;35:57-65.
12. Yamagishi M, Uchimaru K. Targeting EZH2 in cancer therapy. Curr Opin Oncol 2017;29:375-81.
13. Shorstova T, Marques M, Su J, et al. SWI/SNF-Compromised Cancers Are Susceptible to Bromodomain Inhibitors. Cancer Res 2019;79:2761-74.
14. Kawachi H, Kunimasa K, Kukita Y, et al. Atezolizumab with bevacizumab, paclitaxel and carboplatin was effective for patients with SMARCA4-deficient thoracic sarcoma. Immunotherapy 2021;13:799-806.
15. Iijima Y, Sakakibara R, Ishizuka M, et al. Notable response to nivolumab during the treatment of SMARCA4-deficient thoracic sarcoma: a case report. Immunotherapy 2020;12:563-9.
16. Li B, Li XG. Iodine-125 Seed Implantation and Transarterial Chemoinfusion Combined with Immune Checkpoint Inhibitors for a Thoracic SMARCA4-Deficient Undifferentiated Tumor. J Vasc Interv Radiol 2023;34:147-9.
17. Crombé A, Alberti N, Villard N, et al. Imaging features of SMARCA4-deficient thoracic sarcomas: a multi-centric study of 21 patients. Eur Radiol 2019;29:4730-41.
18. Liang X, Gao X, Wang F, et al. Clinical characteristics and prognostic analysis of SMARCA4-deficient non-small cell lung cancer. Cancer Med 2023;12:14171-82.
19. Kezlarian B, Montecalvo J, Bodd FM, et al. Diagnosis of thoracic SMARCA4-deficient undifferentiated tumor in cytology. Cancer Cytopathol 2023;131:526-34.
20. Jiang J, Chen Z, Gong J, et al. Thoracic SMARCA4-deficient undifferentiated tumor. Discov Oncol 2023;14:51.
21. Nambirajan A, Jain D. Recent updates in thoracic SMARCA4-deficient undifferentiated tumor. Semin Diagn Pathol 2021;38:83-9.
22. Lorentzen T, Nolsøe CP, Ewertsen C, et al. EFSUMB Guidelines on Interventional Ultrasound (INVUS), Part I. General Aspects (Short Version). Ultraschall Med 2015;36:464-72.
23. Yi D, Feng M, Wen Ping W, et al. Contrast-enhanced US-guided percutaneous biopsy of anterior mediastinal lesions. Diagn Interv Radiol 2017;23:43-8.
24. Paes FM, Kalkanis DG, Sideras PA, et al. FDG PET/CT of extranodal involvement in non-Hodgkin lymphoma and Hodgkin disease. Radiographics 2010;30:269-91.
25. Kitami A, Sano F, Ohashi S, et al. The Usefulness of Positron-Emission Tomography Findings in the Management of Anterior Mediastinal Tumors. Ann Thorac Cardiovasc Surg 2017;23:26-30.
26. Patnaik S, Malempati AR, Uppin M, et al. Rare mediastinal masses – imaging review. J Cancer Res Ther 2021;17:13-21.
27. Ozawa Y, Hiroshima M, Maki H, et al. Imaging findings

of lesions in the middle and posterior mediastinum. Jpn J Radiol 2021;39:15-31.
28. Carter BW, Benveniste MF, Madan R, et al. ITMIG Classification of Mediastinal Compartments and Multidisciplinary Approach to Mediastinal Masses. Radiographics 2017;37:413-36.
29. Hoppe BS, Advani R, Milgrom SA, et al. Primary Mediastinal B Cell Lymphoma in the Positron-Emission Tomography Era Executive Summary of the American Radium Society Appropriate Use Criteria. Int J Radiat Oncol Biol Phys 2021;111:36-44.
30. Baudin E, Caplin M, Garcia-Carbonero R, et al. Lung and thymic carcinoids: ESMO Clinical Practice Guidelines for diagnosis, treatment and follow-up(☆). Ann Oncol 2021;32:439-51.
31. Rudin CM, Brambilla E, Faivre-Finn C, et al. Small-cell lung cancer. Nat Rev Dis Primers 2021;7:3.
32. Wang Q, Gümüş ZH, Colarossi C, et al. SCLC: Epidemiology, Risk Factors, Genetic Susceptibility, Molecular Pathology, Screening, and Early Detection. J Thorac Oncol 2023;18:31-46.
33. Chatzopoulos K, Boland JM. Update on genetically defined lung neoplasms: NUT carcinoma and thoracic SMARCA4-deficient undifferentiated tumors. Virchows Arch 2021;478:21-30.
34. Ribeiro JA, Sousa J, Jesus F, et al. NUT carcinoma – An aggressive thoracic tumor. Am J Med Sci 2023;366:64-70.
35. Yoshida A. NUT carcinoma and thoracic SMARCA4-deficient undifferentiated tumour: facts and controversies. Histopathology 2024;84:86-101.
36. Wang D, Zhang J, Liu Y, et al. Diagnostic Value of Transthoracic Echocardiography Combined With Contrast-Enhanced Ultrasonography in Mediastinal Masses. J Ultrasound Med 2019;38:415-22.
37. Yan L, Ruan Q, Qu C, et al. The value of transthoracic echocardiography in the detection of extra-cardiac lesions. BMC Surg 2022;22:73.
38. Pan J, Chen W, Zhang H, et al. Contrast-Enhanced Ultrasonography versus Contrast-Enhanced Magnetic Resonance Imaging in the Diagnosis of Mediastinal Tumors. Ultrasound Med Biol 2021;47:261-71.
39. Kong J, Fu JJ, Yang W, et al. Contrast-enhanced ultrasound features of mediastinal lymphomas and thymic epithelial tumors. J Clin Ultrasound 2020;48:19-28.
40. Kuwamoto S, Matsushita M, Takeda K, et al. SMARCA4-deficient thoracic sarcoma: report of a case and insights into how to reach the diagnosis using limited samples and resources. Hum Pathol 2017;70:92-7.
41. Cao BS, Wu JH, Li XL, et al. Sonographically guided transthoracic biopsy of peripheral lung and mediastinal lesions: role of contrast-enhanced sonography. J Ultrasound Med 2011;30:1479-90.
42. Trenker C, Dietrich CF, Holland A, et al. Mediastinal Masses in Contrast-Enhanced Ultrasound – Retrospective Analysis of 58 Cases. J Ultrasound Med 2021;40:1023-30.
43. Liang J, Wang D, Li H, et al. Contrast-enhanced ultrasound for needle biopsy of thoracic lesions. Oncol Lett 2020;20:75.

Cite this article as: Yang D, Wang Y. Imaging performance of thoracic SMARCA4-deficient undifferentiated tumor: a case report and literature review. Transl Lung Cancer Res 2024;13(2):443-452. doi: 10.21037/tlcr-23-822